Appl Microbiol Biotechnol (2007) 75:999–1005
DOI 10.1007/s00253-007-0899-7

Unique butyric acid incorporation patterns for salinosporamides A and B reveal distinct biosynthetic origins

Ginger Tsueng · Katherine A. McArthur · Barbara C. M. Potts · Kin S. Lam

Received: 23 October 2006 / Revised: 15 February 2007 / Accepted: 19 February 2007 / Published online: 6 March 2007

Abstract Feeding sodium butyrate (0.25–1 mg/ml) to cultures of *Salinispora tropica* NPS21184 enhanced the production of salinosporamide B (NPI-0047) by 319% while inhibiting the production of salinosporamide A (NPI-0052) by 26%. Liquid chromatography mass spectrometry analysis of the crude extract from the strain NPS21184 fed with 0.5 mg/ml sodium [U-$^{13}C_4$]butyrate indicated that butyrate was incorporated as a contiguous four-carbon unit into NPI-0047 but not into NPI-0052. Nuclear magnetic resonance analysis of NPI-0047 and NPI-0052 purified from the sodium [U-$^{13}C_4$]butyrate-supplemented culture extract confirmed this incorporation pattern. The above finding is the first direct evidence to demonstrate that the biosynthesis of NPI-0047 is different from NPI-0052, and NPI-0047 is not a precursor of NPI-0052.

Keywords *Salinispora tropica* · Salinosporamides · Biosynthesis · Butyric acid

Introduction

Salinosporamide A (NPI-0052) is a small molecule natural product isolated from marine actinomycete *Salinispora tropica* (Feling et al. 2003). It is a highly potent inhibitor of the 20S proteasome (Chauhan et al. 2005; Groll et al. 2006) and is currently undergoing phase I clinical studies for the treatment of various cancers. NPI-0052 comprises a fused γ-lactam-β-lactone ring system that is decorated with a cyclohexenyl carbinol at the C-4 ring junction, a chloroethyl substituent at C-2, and a methyl group at the C-3 ring junction (Fig. 1). The structural components are suggestive of mixed biosynthetic origin; the cyclohexenyl carbinol unit joined to the Cα carbon (C-4) and juxtaposed between the lactam NH and the β-lactone carbonyl is reminiscent of a modified phenylalanine, suggesting that it is derived from an aromatic amino acid pathway, whereas the remainder of the molecule is putatively derived from polyketide biosynthesis. The structures of other naturally occurring analogs of NPI-0052 indicated that the greatest diversity in the analog pool occurred at the C-2 substituent. To date, the naturally occurring analogs that have been identified in the C-2 substituent series include methyl, ethyl and propyl, and C-2 epimers of the chloroethyl, methyl, and ethyl analogs (Macherla et al. 2005; Williams et al. 2005; Reed et al. 2007).

We have developed fermentation conditions in our laboratory under which NPI-0052 is the major salinosporamide metabolite in the production culture of *S. tropica* NPS21184 with a titer of about 400 mg/l. Salinosporamide B (NPI-0047; Fig. 1), the deschloro analog, is the second most abundant secondary metabolite produced during fermentation and interferes with the purification of NPI-0052. Thus, reducing or eliminating the production of NPI-0047 in the fermentation would significantly enhance the recovery of NPI-0052 during the large scale manufacturing process. Although it is conceivable that NPI-0047 is a direct precursor of NPI-0052, under those circumstances, it would be very difficult to devise biosynthetic schemes to specifically inhibit the production of NPI-0047 without lowering the production of NPI-0052; the only logical approach would be to enhance the activity of the enzyme, a halogenase, in *S. tropica* to optimize the conversion of NPI-0047 to NPI-0052.

G. Tsueng · K. A. McArthur · B. C. M. Potts · K. S. Lam (✉)
Nereus Pharmaceuticals,
10480 Wateridge Circle,
San Diego, CA 92121, USA
e-mail: rlam@nereuspharm.com

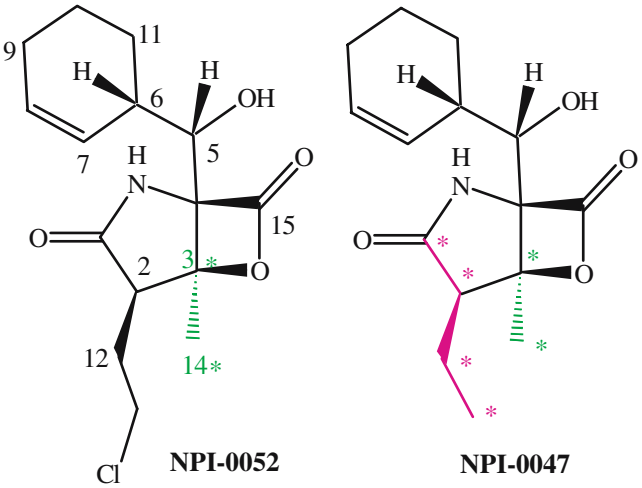

Fig. 1 Structure of NPI-0052 and NPI-0047

Elucidation of the biosynthesis of salinosporamides by *S. tropica* is expected to be advantageous in many regards, including: (1) providing a means to improve the production of NPI-0052 and desirable analogs; (2) decreasing the production of undesirable analogs (such as NPI-0047); (3) establishing conditions for generating novel analogs; and (4) providing the optimal route for the preparation of isotopically labeled drug metabolites for pharmacokinetic studies. We were particularly interested in deducing the biosynthetic origin of the contiguous four-carbon unit C-1, C-2, C-12, and C-13 of NPI-0047 and NPI-0052 as this moiety represents the greatest diversity in the biosynthetic analog pool and offers potential to provide practical solutions to the problems outlined above.

Materials and methods

Microorganism

The producing strain, *S. tropica* NPS21184, is a single colony isolate of the wild type strain, NPS465. Strain NPS465 was isolated from a sediment sample collected from Cross Harbor, Abaco, Bahamas (Jensen et al. 1991). Strains NPS465 and NPS21184 were deposited with the American Type Culture Collection and assigned the accession number PTA-5275 and PTA-6685, respectively.

Growth media and culturing conditions

To prepare inoculum for shake flask culture, a frozen stock culture was transferred to a 500-ml Erlenmeyer flask containing 100 ml of seed medium consisting of the following ingredients per liter of deionized water: 8 g of glucose (Sigma), 6 g of Hy Soy (Kerry Biosciences), 6 g of yeast extract (USB), and 30 g of Instant Ocean (Aquarium Systems). The first seed culture was incubated at 28°C and 250 rpm on a rotary shaker. After 3 days, a 5-ml aliquot of the first seed culture was inoculated into a 500-ml Erlenmeyer flask containing 100 ml of the same seed medium. The second seed culture was incubated at 28°C and 250 rpm on a rotary shaker for 2 days. Five-milliliter aliquots of second seed cultures were then transferred to 500-ml Erlenmeyer flasks containing 100 ml of production medium consisting of the following ingredients per liter of deionized water: 10 g of starch (USB), 4 g of Hy Soy, 4 g of yeast extract, 1 g $CaCO_3$ (Sigma), 0.04 g $Fe_2(SO_4)_3$ (Aldrich), 0.1 g KBr (Fisher), and 30 g of Instant Ocean. After 2 days of incubation at 28°C and 250 rpm, various amounts of sodium butyrate (Aldrich) were added to the production cultures to yield final concentrations of 0.25–1 mg/ml. One hour after the addition of sodium butyrate, 2 g of Amberlite XAD-7 (Sigma) resin was added to the production culture. The production cultures were further incubated at 28°C and 250 rpm for additional 2–3 days to complete the production cycle of salinosporamides.

For the [U-$^{13}C_4$]butyrate enrichment study, 100 mg of sodium [U-$^{13}C_4$]butyrate (Aldrich) was dissolved in deionized water (2 ml) and filter sterilized through a 0.2-μm Acrodisc syringe filter (Pall). At 47 h in the production cycle, 1 ml of the [U-$^{13}C_4$]butyrate solution was added to each of the two production flasks, and 2 g of Amberlite XAD-7 resin was added 1 h after the addition of [U-$^{13}C_4$]butyrate. The culture was extracted at day 4 of the production cycle.

Growth analysis

The growth of the culture was determined by centrifuging 10 ml of culture in a 15-ml centrifuge tube at 3,000 rpm for 15 min in a Beckman centrifuge (Allegra model 6). The growth of the culture was expressed as percent packed cell volume defined as the volume of packed cell/volume of culture×100%.

Extraction and analytical methods

The production of salinosporamides in the fermentation was monitored by Agilent HP1100 high-performance liquid chromatography (HPLC) using an ACE C-18 reversed-phase column (4.6×150 mm) and a solvent system consisting of water (0.01% TFA) as solvent A and acetonitrile (0.01% TFA) as solvent B. The elution profile was as follows: 100% solvent A for 1 min followed by a linear gradient to 35% solvent A in 7 min, held at 35% solvent A for 11 min, followed by a linear gradient to 100% solvent B in 8 min, held at 100% solvent B for 9 min at a flow rate of 1.5 ml/min with the detector wavelength set at 210 nm and column temperature at 35°C. The fermentation

extract for the HPLC analysis was prepared by extracting culture broth (3.5 ml) with an equal volume of ethyl acetate for 1 h. A 1-ml aliquot was evaporated to dryness under a stream of nitrogen and redissolved in 320 μl of dimethyl sulfoxide (DMSO). Five microliters of the extract was used for HPLC analysis. For the liquid chromatography mass spectrometry (LC-MS) analysis of the crude extract and purified compounds, an Agilent HP1100 HPLC equipped with an Agilent PDA detector and a 1100 series MSD Agilent mass spectrometer was used, along with the same mobile and stationary phase and elution profile as described above.

Purification of NPI-0047 and NPI-0052 from sodium [U-$^{13}C_4$]butyrate-supplemented culture of strain NPS21184

The [U-$^{13}C_4$]butyrate-fed culture (~200 ml) was filtered through a cheesecloth to recover the resin. The resin was placed in a 500-ml flask containing 200 ml of ethyl acetate and agitated at 250 rpm on a rotary shaker for 1 h. The extract was filtered through a Whatman no. 4 filter paper, and the filtered extract was dried in vacuo to yield 46 mg of dried extract. The crude extract was purified by HPLC using a Gilson HPLC equipped with a Gilson 215 fraction collector and an evaporative light scattering detector (ELSD, Sedere) to monitor the purification process. The extract was dissolved in acetone to a final concentration of 40 mg/ml, filtered through a 0.45-μm syringe filter and purified by HPLC using a normal phase silica column (Phenomenex Luna Si 10 μm, 250× 21.2 mm id). The mobile phase elution profile was 24% ethyl acetate/hexanes for 27 min, 24% ethyl acetate/hexanes to 100% ethyl acetate in 1 min, followed by 100% ethyl acetate for 11 min at a flow rate of 25 ml/min. NPI-0052 was eluted as a broad peak between 14 and 19 min, and NPI-0047 was eluted at 31 min as a pure compound.

NMR analysis of NPI-0047 and NPI-0052

^{1}H and ^{13}C NMR spectra were collected using a 500-MHz Bruker Avance NMR spectrometer with a broadband observe probe. All NMR data were acquired at 300 K in DMSO-d_6. The enrichment factor was calculated as follows: The ^{13}C-NMR spectrum of the natural abundance standard was acquired, and the peak area for each carbon of interest was integrated against that of C-10, which was calibrated to a unit of 1. This established the ratio of peak intensities in the natural abundance standard to take relaxation, NOE, and other factors that affect relative peak intensity into consideration. The ^{13}C-NMR spectrum of the ^{13}C-enriched sample was then acquired, and the peak area for each carbon of interest was again integrated against C-10 (calibrated to 1; note: no ^{13}C-enrichment was observed for this carbon) and then corrected according to the peak ratio established in the natural abundance spectrum. Further details specific to each carbon can be found in Table 2.

Results

Effect of sodium butyrate on the production of salinosporamides

Butyric acid is incorporated as a whole four-carbon unit into many antibiotics, including ascomycin (Byrne et al. 1993), tylosin (Omura et al. 1976; Rezanka et al. 1991), leucomycin (Omura et al. 1977), turimycin (Gersch et al. 1977), lasalocid A (Sherman and Hutchinson 1987), and monensin A (Pospisil et al. 1985). As the contiguous four-carbon unit C-1, C-2, C-12, and C-13 of NPI-0047 and NPI-0052 might be derived from butyric acid, we examined the effect of different concentrations of sodium butyrate on the production of salinosporamides by *S. tropica* NPS21184, and the findings are summarized in Table 1. To our surprise, we observed that butyrate significantly enhanced the production of NPI-0047 but inhibited the production of NPI-0052. The enhancement of NPI-0047 production by butyrate was concentration dependent, with maximal production of NPI-0047 at 1 mg/ml of butyrate, which gave rise to a titer of 49.9 mg/l, representing a 319% increase in titer compared with the control (no butyrate, 11.9 mg/l). Even at the lowest butyrate concentration tested at 0.25 mg/ml, the production of NPI-0047 was 32.7 mg/l, a 175% improvement over the control. The optimal inhibition

Table 1 Effect of sodium butyrate on the production of salinosporamides in *S. tropica* NPS21184

Sodium butyrate (mg/ml)	NPI-0047		NPI-0052	
	Maximum titer (mg/l)[a]	Increase (%)	Maximum titer (mg/l)[a]	Decrease (%)
0	11.9	–	279	–
0.25	32.7	175	211	24
0.5	47.1	296	219	22
1	49.9	319	207	26

[a] The maximum titer of the production cycle from day 3 to 5 was reported. The maximum titer usually achieved at day 4 of the production cycle.

Table 2 [U-$^{13}C_4$]butyrate incorporation into NPI-0047 and NPI-0052

Position enriched	Enrichment factor (NPI-0047)	Enrichment factor (NPI-0052)
1	75[a]	Not applicable
2	82[a]	Not applicable
3	13[c]	8[d]
12	70[a]	Not applicable
13	75[a]	Not applicable
14	15[b]	9[d]

In the case of C-3 and C-14, incorporation occurs as a result of breakdown of [U-$^{13}C_4$]butyrate into [1,2-$^{13}C_2$]acetate.

[a] For C-1 and C-13, the peak area for the natural abundance singlet, together with the species that corresponds to incorporation of [1,2-$^{13}C_2$]acetate[e], represented ~2% of the total peak area. We therefore applied this finding to contiguous carbons C-2 and C-12 for which the multiplet structures precluded independent integration of the natural abundance/[1,2-$^{13}C_2$]acetate-incorporated species. Because of this relatively minor contribution to the peak area, the peak integration represents total peak area for all species.

[b] The natural abundance signal, which is coincident with the species that corresponds to incorporation of [U-$^{13}C_4$]butyrate only[e], was not included in the peak integration for determination of enrichment factor. The enrichment factor is based upon integration of the resolved multiplet that arises from two species, which contain [1,2-$^{13}C_2$]acetate or [U-$^{13}C_4$]butyrate plus [1,2-$^{13}C_2$]acetate.

[c] The multiplet structure of C-3 is described in detail in the text. The total peak area was integrated and then corrected based on the percentage of natural abundance/"[U-$^{13}C_4$]butyrate-only" species (i.e., for which [1,2-$^{13}C_2$]acetate was not incorporated) as determined for the contiguous carbon, C-14. The result reflects the enrichment factor for two species, which contain [1,2-$^{13}C_2$]acetate or [U-$^{13}C_4$]butyrate plus [1,2-$^{13}C_2$]acetate.

[d] The natural abundance signal was well resolved from the flanking, enriched doublet and was therefore not included in the peak integration for determination of enrichment factor

[e] Where possible, we have identified the various species that contribute to signal intensity that is coincident with the true natural abundance peak. In the case of the signals for C-1 and C-13 of NPI-0047, the species that corresponds to incorporation of [1,2-$^{13}C_2$]acetate is coincident with the natural abundance peak, whereas the other species, which contain [U-$^{13}C_4$]butyrate only or [U-$^{13}C_4$]butyrate plus [1,2-$^{13}C_2$]acetate, are resolved. In the case of the C-14 signal of NPI-0047, the species that corresponds to incorporation of [U-$^{13}C_4$]butyrate is coincident with the natural abundance peak. The cases of C-2, C-12, and C-3 are more complex, and the latter is discussed in detail in the text

of NPI-0052 was observed at around 0.25 mg/ml of butyrate, decreasing production by 24%. Sodium butyrate, at the concentrations tested, did not affect the growth of *S. tropica* as the percent packed cell volume was very similar between the control culture and the butyrate-supplemented cultures at about 6%.

LC-MS analysis of crude extract from sodium [U-$^{13}C_4$] butyrate-supplemented culture of strain NPS21184

A crude extract generated from sodium [U-$^{13}C_4$]butyrate-supplemented culture of strain NPS21184 was analyzed by LC-MS to determine the incorporation of [U-$^{13}C_4$]butyrate into NPI-0047 (Fig. 2). The molecular ion (*m/z* 284 $[M+H+4]^+$) of NPI-0047 from the [U-$^{13}C_4$]butyrate-fed culture was four mass units higher than the molecular ion of NPI-0047 observed in the control culture, supporting the incorporation of [U-$^{13}C_4$]butyrate into NPI-0047. The amount of ^{13}C-labeled NPI-0047 present in the [U-$^{13}C_4$] butyrate-fed culture was estimated to be sixfold from that of NPI-0047 present in the control culture based on the signal intensity from the mass spectrum (7937 versus 1300). Although we have not established the relationship of signal intensity from the mass spectrum to the concentration of NPI-0047, the estimated sixfold increase in NPI-0047 concentration in the [U-$^{13}C_4$]butyrate-fed culture correlates well with the fourfold (296%) increase in the NPI-0047 concentration, determined by HPLC analysis, when the same amount of unlabeled butyrate (0.5 mg/l, Table 1) was added to the culture. Two molecular ions were also observed at *m/z* 282 $[M+H+2]^+$ and *m/z* 286 $[M+H+6]^+$ for NPI-0047 from the [U-$^{13}C_4$]butyrate-fed culture but not in the control culture. It was proposed that these ions might correspond to the enrichment of the two carbons at the C-3 ring juncture and C-14 methyl moiety, as [U-$^{13}C_4$]butyrate could be broken down into [1,2-$^{13}C_2$]acetate and then incorporated into NPI-0047 with (*m/z* 286 $[M+H+6]^+$) or without (*m/z* 282 $[M+H+2]^+$) the incorporation of [U-$^{13}C_4$] butyrate. NPI-0052 from the crude extracts of sodium [U-$^{13}C_4$]butyrate-supplemented culture and the control culture gave rise to the same major observed ion (*m/z* 314 $[M+H]^+$), indicating that butyrate did not incorporate into NPI-0052.

Purification of NPI-0047 and NPI-0052 from sodium [U-$^{13}C_4$]butyrate-supplemented culture of strain NPS21184

Preparative HPLC was used to process the extract (46 mg) generated from a 200-ml *S. tropica* culture fed with 0.5 mg/ml of sodium [U-$^{13}C_4$]butyrate at 46 h of the production cycle. The whole filtered extract was injected onto the preparative HPLC and resulted in the recovery of 12.1 mg NPI-0052 and 4.1 mg NPI-0047, both of which were greater than 95% purity when analyzed by proton NMR.

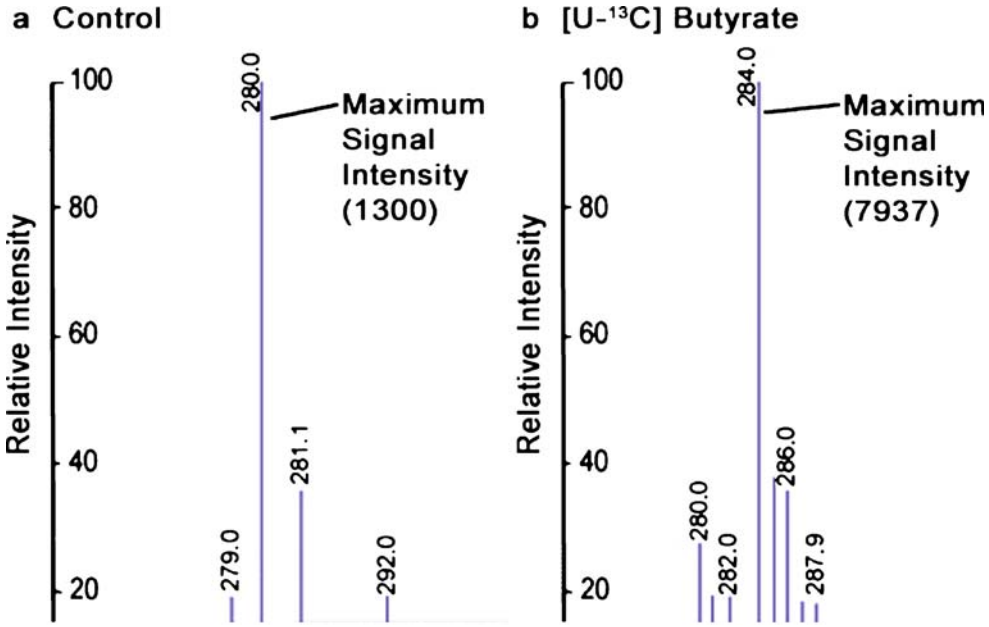

Fig. 2 LC-MS analysis of NPI-0047 in crude extract of control culture (**a**) and [U-$^{13}C_4$]butyrate-fed culture (**b**) of *S. tropica* NPS21184

LC-MS and NMR analyses of NPI-0047 and NPI-0052 isolated from sodium [U-$^{13}C_4$]butyrate-supplemented culture of strain NPS21184

LC-MS analysis of purified NPI-0047 and NPI-0052 from the [U-$^{13}C_4$]butyrate-fed culture yielded similar results to those obtained from the crude extract. A major molecular ion of *m/z* 284 $[M+H+4]^+$ along with a second ion of *m/z* 286 $[M+H+6]^+$ were observed in the LC-MS of NPI-0047. For NPI-0052, the unlabelled species gave rise to the major observed ion {*m/z* 314 ($[M+H]^+$)}; however, the [1,2-$^{13}C_2$] acetate labeled species was also present, increasing the intensity of the ion at *m/z* 316 ($[M+H+2]^+$), which is coincident with the ^{37}Cl isotope of the unlabeled parent.

NMR analysis of NPI-0047 isolated from the [U-$^{13}C_4$] butyrate-fed culture confirmed the enrichment of ^{13}C at all carbons of the contiguous four-carbon unit C-1, C-2, C-12, and C-13 with an enrichment factor of 76±6 as shown in Table 2. The relative peak intensities, together with the observed coupling constants, supported the incorporation of an intact [U-$^{13}C_4$]butyrate within the molecule. C-1, a doublet of doublets, had both short and long range

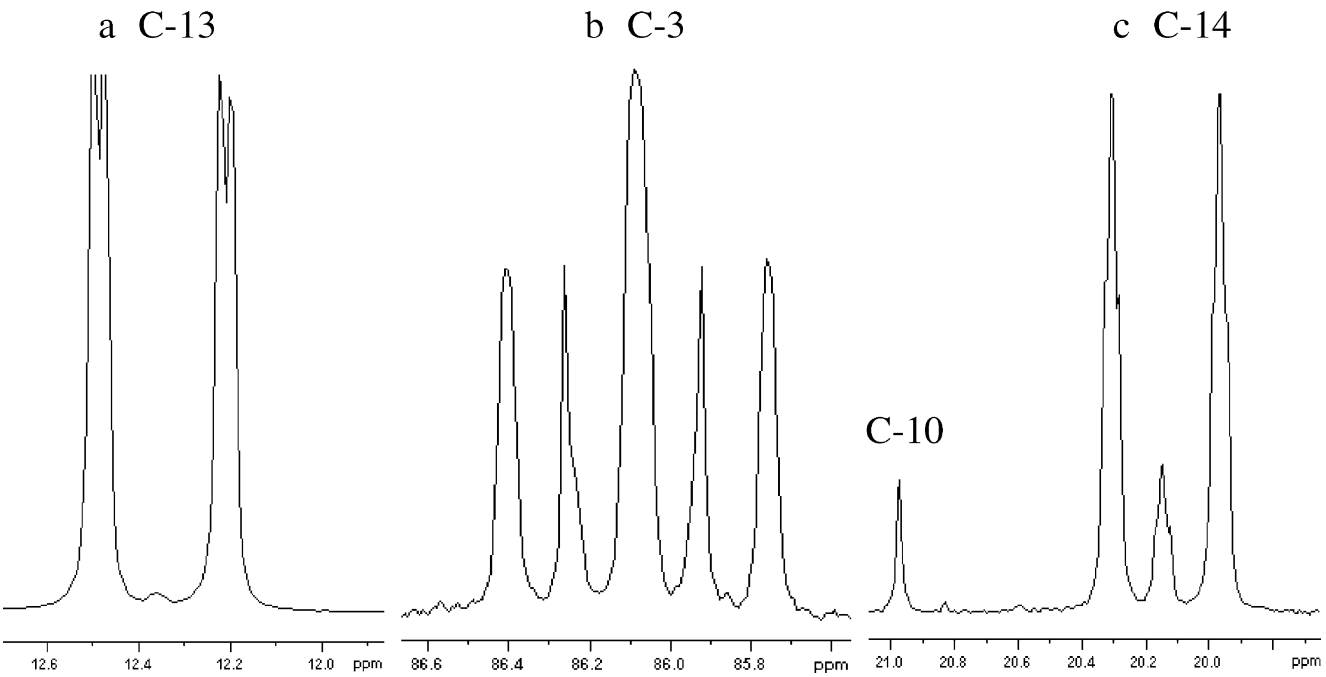

Fig. 3 Expansions of ^{13}C NMR spectrum of NPI-0047 showing multiplet structures of C-13 (**a**), C-3 (**b**), and C-14 (**c**) with *labeled peaks* flanking the natural abundance signal and the unlabeled C-10 signal shown for reference

couplings to C-2 and C-12, respectively (δ_{C1} 175.8; $J_{1,2}$= 47 Hz, $J_{1,12}$=4 Hz). A similar pattern was observed for the terminal methyl group C-13 (δ_{C13} 12.4; dd, $J_{13,12}$=35 Hz, $J_{13,2}$=4 Hz; Fig. 3a). The signal intensities and multiplicities for C-2 (δ_{C2} 49.1; dd, $J_{2,1}$=47 Hz, $J_{2,12}$=36 Hz) and C-12 (δ_{C12} 18.0; dd, $J_{12,2}$=36 Hz, $J_{12,13}$=35 Hz) further indicated that the labeled carbons comprise a contiguous chain. In addition to observing ^{13}C incorporation into the C-1, C-2, C-12, and C-13 chain, the C-3 and C-14 carbon resonances were slightly amplified in the ^{13}C-NMR spectrum, indicating partial incorporation of [1, 2-$^{13}C_2$] acetate derived from [U-$^{13}C_4$]butyrate. The complex multiplet structure of the C-3 signal (Fig. 3b) revealed the presence of three distinctly labeled species of NPI-0047 as follows: one with dual incorporation of [U-$^{13}C_4$]butyrate and [1, 2-$^{13}C_2$] acetate, a second in which only [1,2-$^{13}C_2$] acetate was incorporated, and the third representing the species containing only [U-$^{13}C_4$]butyrate. The first species, with dual incorporation of [U-$^{13}C_4$]butyrate and [1, 2-$^{13}C_2$] acetate, is evident from the amplified "triplet" (br dd), in which C-3 (δ_{C3} 86.1) exhibits two large couplings of similar magnitude (40–43 Hz) to C-2 and C-14. This signal was superimposed with a doublet for which each component displayed an asymmetrical peak shape that was suggestive of the presence of two unique but overlapping species. The intensity of this signal was consistent with the presence of the species in which only [1, 2-$^{13}C_2$] acetate is incorporated (δ_{C3} 86.1; $J_{3,14}$=42 Hz), together with the third species containing only [U-$^{13}C_4$]butyrate (δ_{C3} 86.1; $J_{3,2}$ ~40 Hz) that contributes the shoulder of the doublet that leads to the peak asymmetry. The C-14 methyl signal appeared as a broad doublet (δ_{C14} 20.1; d, $J_{14,3}$=42 Hz) flanking the weaker signal arising from the natural abundance species that is coincident with the species containing only [U-$^{13}C_4$]butyrate (Fig. 3c); the fine structure of the signals can be explained by detailed coupling constant analysis of the contributing, overlapping species. NMR analysis of NPI-0052 purified from the same extract showed enrichment of two doublets corresponding to C-3 (δ_{C3} 85.3; $J_{3,14}$=43) and C-14 (δ_{C14} 19.2; $J_{14,3}$=43) but not the contiguous C-1, C-2, C-12, and C-13 chain (Table 2). These results strongly indicate that butyrate is not a precursor to the chloroethyl side chain of NPI-0052.

Discussion

In this paper, we present the first direct evidence, using a [U-$^{13}C_4$]butyrate feeding study, that the biosynthesis of NPI-0047 is different from NPI-0052. NPI-0047 is biosynthesized via butyrate to form the contiguous carbon chain of C-1, C-2, C-12, and C-13. The same four-carbon contiguous chain in NPI-0052 is not derived from butyrate. Therefore, NPI-0047 is not the direct precursor of NPI-0052 as might have been predicted based on the structures and the current knowledge of the biosynthetic schemes. This is an important finding as we can now devise biosynthetic schemes, such as inactivation of crotonyl-CoA reductase, to cut off the supply of butyrate (Liu and Reynolds 2001) to specifically decrease the production of the NPI-0047 without affecting the production of NPI-0052 in the fermentation. This would not be possible if NPI-0047 was the direct precursor of NPI-0052. As NPI-0047 can interfere with the purification of NPI-0052, reducing or eliminating NPI-0047 from the fermentation would significantly improve the recovery yield of NPI-0052. It is also interesting that the formation of the four-carbon contiguous chain in NPI-0052 is derived from a new biosynthetic route that currently requires further investigation.

We observed that feeding butyrate into the culture of *S. tropica* at a concentration of 1 mg/l increased the production of NPI-0047 by 319% because of a precursor-directed biosynthesis effect. At the same time, butyrate inhibited the production of NPI-0052 by 26%, suggesting that butyrate is competing with the corresponding precursor of NPI-0052 for incorporation into the core of salinosporamide. Therefore, it will be important to determine the precursor for the four-carbon unit of NPI-0052. Enhancing the intracellular level of this four-carbon precursor should enhance the production of NPI-0052. The observation that the two carbons C-3 and C-14 of both NPI-0047 and NPI-0052 were enriched slightly by the [U-$^{13}C_4$]butyrate-fed cultures can be explained by the fact that the ^{13}C-labeled butyrate broke down to form two labeled acetates, which then incorporated as a whole unit into C-3 and C-14.

Our findings also demonstrated the importance of using MS as a tool for analysis of labeled samples from the biosynthetic studies. Analysis of a small amount (~5 μg) of a crude extract from the [U-$^{13}C_4$]butyrate-fed culture by LC-MS using a single quad mass spectrometer clearly indicated that the whole butyrate unit incorporated into NPI-0047 but not NPI-0052. LC-MS analysis can be used as a prescreen system for determining the potential incorporation of labeled precursors into the desired metabolites in small scale before scaling up to obtain a larger quantity for NMR analysis.

References

Byrne KM, Shafiee A, Nielsen J, Arison B, Monaghan RL, Kaplan L (1993) The biosynthesis and enzymology of an immunosuppressant, immunomycin, produced by *Streptomyces hygroscopicus var. ascomyceticus*. Dev Ind Microbiol 32:29–45

Chauhan D, Catley L, Li G, Podar K, Hideshima T, Velankar M, Mitsiades C, Mitsiades N, Yasui H, Letai A, Ovaa H, Berkers C,

Nicholson B, Chao TH, Neuteboom STC, Richardson P, Palladino MA, Anderson KC (2005) A novel orally active proteasome inhibitor induces apoptosis in multiple myeloma cells with mechanisms distinct from Bortezomib. Cancer Cell 8:407–419

Feling RH, Buchanan GO, Mincer TJ, Kauffman CA, Jensen PR, Fenical W (2003) Salinosporamide A: a highly cytotoxic proteasome inhibitor from a novel microbial source, a marine bacterium of the new genus *Salinispora*. Angew Chem Int Ed Engl 42:355–357

Gersch D, Bocker H, Thrum H (1977) Biosynthetic studies on the macrolide antibiotic turimycin using ^{14}C-labeled precursors. J Antibiot 30:488–493

Groll M, Huber R, Potts BCM (2006) Crystal structures of salinosporamide A (NPI-0052) and B (NPI-0047) in complex with the 20S proteasome reveal important consequences of beta-lactone opening and a mechanism for irreversible binding. J Am Chem Soc 128:5136–5141

Jensen PR, Dwight R, Fenical W (1991) Distribution of actinomycetes in near-shore tropical marine sediments. Appl Environ Microbiol 57:1102–1108

Liu H, Reynolds KA (2001) Precursor supply for polyketide biosynthesis: the role of crotonyl-CoA reductase. Metab Eng 3:40–48

Macherla VR, Mitchell SS, Manam RR, Reed KA, Chao T, Nicholson B, Deyanat-Yazdi G, Mai B, Jensen PR, Fenical WF, Neuteboom STC, Lam KS, Palladino MA, Potts BCM (2005) Structure-activity relationship studies of NPI-0052, a novel marine derived 20S proteasome inhibitor. J Med Chem 48:3684–3687

Omura S, Takeshima H, Nakagawa A, Kanemoto N, Lukacs G (1976) Studies on carboxylic acid metabolism in a macrolide-producing microorganism using carbon-13 magnetic resonance. Bioorg Chem 5:451–454

Omura S, Takeshima H, Nakagawa A, Miyazawa J, Piriou F, Lukacs G (1977) Studies on the biosynthesis of 16-membered macrolide antibiotics using carbon-13 nuclear magnetic resonance spectroscopy. Biochemistry 16:2860–2866

Pospisil S, Cimburkova E, Krumphanzl V, Vanek Z (1985) Effect of precursors on biosynthesis of monensins A and B. Folia Microbiol 30:30–33

Reed KA, Manam RR, Mitchell SS, Xu J, Teisan S, Chao TH, Deyanat-Yazdi G, Neuteboom STC, Lam KS, Potts BCM. (2007) Salinosporamides D-J from the marine actinomycete *Salinispora tropica*, bromosalinosporamide, and thioester derivatives are potent inhibitors of the 20S proteasome. J Nat Prod 70:269–276

Rezanka T, Reichelova J, Kopecky J (1991) Isobutyrate as a precursor of *n*-butyrate in the biosynthesis of tylosin and fatty acids. FEMS Microbiol Lett 68:33–36

Sherman MM, Hutchinson CR (1987) Biosynthesis of lasalocid A: biochemical mechanism for assembly of the carbon framework. Biochemistry 26:438–445

Williams PG, Buchanan GO, Feling RH, Kauffman CA, Jensen PR, Fenical W (2005) New cytotoxic salinosporamides from the marine actinomycete *Salinispora tropica*. J Org Chem 70:6196–6203